# STUDY ON DROPLET DEPOSITION IN PWM FLOW-CONTROLLED SPRAYING UNDER VARIABLE PRESSURE

1

PWM 调压控流喷雾的液滴沉积研究

Yang MA 1), Huimei ZHANG \*1), Lei SHU 2), Yue ZHANG 3)

¹)Chongqing Medical and Pharmaceutical College, Chongqing / China ²)Southwest University, Chongqing /China ³)Electric Connector Technology Co., Ltd, Chongqing /China Tel: +86-18502316382; E-mail: may\_swu@163.com Corresponding author: Huimei Zhang DOI: https://doi.org/10.35633/inmateh-77-47

Keywords: spray, variable pressure and flow control, CFD simulation, atomization characteristic, deposition

#### **ABSTRACT**

The utilization rate of pesticides in China is low, which causes much pesticide waste and serious pollution of the ecological environment. The main reason of this problem is that the deposition rate of spray is not fairly high and the most fundamental factors affecting droplet deposition are the speed of droplet movement and the size of droplet particles. This study establishes a PWM intermittent spray system under variable pressure and flow control. Through CFD simulations, the atomization characteristics of the nozzle are analyzed. The results indicate that the system can generate finer droplet sizes and higher droplet velocities. By constructing a measurement platform for droplet experiments, tests are conducted on droplet sizes at different horizontal positions under four pressure levels: 0.3 MPa, 0.4 MPa, 0.5 MPa, and 0.6 MPa. The results indicate that as the spray pressure increases, the droplets exhibit a significant tendency to disperse toward both sides, and the droplet size decreases significantly. The field experiment is conducted with broad bean in flowering period. The results show that the average deposition rate increases by 9.9%, 26.4% and 22.9% when the spray pressure is 0.4 MPa, 0.5 MPa and 0.6 MPa compared with 0.3 MPa. This paper verifies the feasibility of the system in improving the spray pressure and quantitatively controlling the spray flow rate, and improving the deposition of droplets by obtaining finer particle size and higher spray velocity. In this sense, this paper has a certain reference significance for improving the effective utilization rate of pesticides and protecting the environment.

#### 摘要

我国农药的利用率低,在造成农药大量浪费的同时严重污染了生态环境,其中主要原因就是喷雾沉积率不高导致的。雾滴运动速度和雾滴粒径大小是影响雾滴沉积的最根本因素。本文搭建了PWM间歇式调压控流喷雾控制系统,利用CFD仿真,对喷头的雾化特性进行了分析,结果表明系统能够产生出更细的雾滴粒径,更大的雾滴运动速度;通过搭建雾滴测量平台进行实验,对0.3MPa、0.4MPa、0.5MPa和0.6MPa四个压力下不同水平位置的雾滴粒径进行了测试,结果表明:随着喷雾压力的增大,雾滴向两侧分散的趋势显著,雾滴粒径减小明显。以开花期蚕豆为试验对象,进行了田间实验,结果表明:喷雾压力为0.4MPa、0.5MPa和0.6MPa相比于0.3MPa,平均沉积率增加了9.9%、26.4%、22.9%。本文验证了系统在提高喷雾压力的同时定量控制喷雾流量,通过获得较细的雾滴粒径和更高的雾滴速度,来提高雾滴沉积的可行性,对提高农药的有效利用率,保护环境有一定的参考意义。

## INTRODUCTION

In the atomization process of atomized droplets produced by the nozzle, the main atomization parameters include droplet particle size, droplet velocity and fog cone angle. The droplet velocity and droplet particle diameter are the main factors affecting droplet deposition and drift loss. For different biological targets, the optimal ranges of fog droplet size of pesticides for controlling different types of pests are also different (*Yuan et al., 2015*). The Optimal Droplet Size Theory in biology holds the view that for different biological targets, the most effective pest control can only be achieved when the droplet size falls within the optimal range, as this ensures the maximum number of droplets are captured by the target (*Liu et al., 2022*).

Yang Ma, Lecturer M.S.Eng.; Huimei Zhang, Assoc. Prof. Ph.D.Eng.; Lei Shu, M.S.Eng.; Yue Zhang, M.Ed.;

The research field of atomization characteristics has been explored to a certain degree at home and abroad. Wongsuk et al., (2024), explore the spray atomization characteristics of multi-rotor UAV. The results show that the flat sector nozzle can produce finer droplets and form higher deposition rate. The atomization characteristics of the nozzle are consistent in the downward flow field, but are greatly influenced by the nozzle type and spray pressure. Nukeshev et al., (2024), conduct a study on the atomization characteristics by examining the spray angle and spray velocity. Through computational fluid dynamics (CFD) simulations, the results demonstrate that adjusting parameters such as the spray angle and velocity of flat-fan nozzles could improve spray uniformity to 74%. Koo, Daewon et al., (2024), investigate the effect of spray height on droplet deposition in turfgrass using an agricultural spray drone (ASD). When the spray height is 2 meters, deposition effectiveness surpasses that of a ground sprayer. As the operational height increases, the spray swath widens significantly and droplet drift accrues, while effective application rate and total deposition decreases. Specifically, total deposition is reduced by 6% for every meter increased in ASD operational height. Sapkota, Madan et al., (2023), evaluate the spray deposition and quality of agricultural sprayers with and without flow rate controllers at different ground speeds. The results show the conclusion that as the ground speed increases, spray deposition decreases significantly. Compared to traditional sprayers (without rate controllers), agricultural sprayers which are equipped with rate controllers could provide adequate and consistent spray deposition when ground speed varies during pesticide application. Wang Shilin et al., (2024), analyze the atomization and deposition characteristics of the hydraulic nozzle, and the results show that the particle size of the droplets decreases along with the increase of the spray pressure, and the higher spray pressure has a significant impact on the droplet deposition of the jet hollow cone nozzle. Zhang Ruirui et al., (2019), study the atomization characteristics of pulse-width modulation variable control nozzle, and the results suggest that when the duty ratio is between 10% and 40%, the particle size of fog droplets decreases along with the increase of duty ratio. When the wind speed is 1 m/s, the fog droplets are deposited within 3.3 m away from the nozzle, and the deposition rate is 95.7%. When the wind speed is increased, the drift of fog droplets is higher. To sum up, scholars at home and abroad have studied the atomization characteristics of the nozzle to some extent, however, under different parameter settings, the dosage of spray solution will be increasing according to the corresponding degrees. This paper constructs an experimental study on a PWM intermittent spray system under variable pressure and flow control. Under the premise of not increasing the dosage of liquid, the atomization effect of the nozzle is changed through the change of spray pressure, atomizing different particle size threshold and different droplet movement speed, so as to improve the deposition rate of the spray liquid on the leaf surface of the crop, and this can guide the actual application in the field. This system operates through control algorithms, offering certain economic and environmental advantages over previous methods where predecessor scholars improve deposition rates by adding devices (such as electrostatic spraying) or auxiliary agents for spraying.

## **MATERIALS AND METHODS**

## System overview

The overall system architecture is shown in Fig. 1. Functionally, it mainly includes: power module, sensor detection module, actuator module, controller module, etc. The sensor module is composed of a level sensor, a pressure transmitter and a flow sensor. It collects spray state parameters in the pipeline and returns the collected signals to the controller. The controller judges the signals and then controls the actuator to complete corresponding actions. The actuator module mainly includes DC electric diaphragm pump, high-speed switch solenoid valve and overflow valve. The controller module is mainly composed of STM32F103 single chip microcomputer and peripheral circuit, and its main functions include two parts: (1) as a detection unit, the single chip microcomputer receives the switching value signal output by the liquid level sensor through the control circuit, the analog voltage signal output by the pressure transmitter and the flow sensor, and the detected signal serves as the decision-making basis for the controller to control the action of the actuator; (2) as a signal output unit, it generates high and low level control signals, which are provided to the DC electric diaphragm pump and high-speed switch solenoid valve through the corresponding control circuit to ensure coordinated operation between the diaphragm pump and high-speed switch solenoid valve achieve variable pressure and flow control.

PWM control technology is employed to adjust the armature voltage by varying the duty cycle of the semiconductor drive signal. This regulates the effective armature voltage of the DC motor in the diaphragm pump, thereby increasing the motor speed. As the speed increases, the reciprocating frequency of the dual-mode mechanism driven by the eccentric plate also increases, which raises the pipeline pressure.

However, increasing the motor speed also increases the spray flow rate. Therefore, the valve switching of the high-speed solenoid valve is simultaneously controlled using a second pulse signal with an adjustable duty cycle to regulate the flow. By coordinating the DC motor speed with the switching frequency of the high-speed solenoid valve, both the spray flow rate and pipeline pressure are precisely controlled, allowing adjustment of the fog droplet size, droplet fineness, and droplet movement velocity.

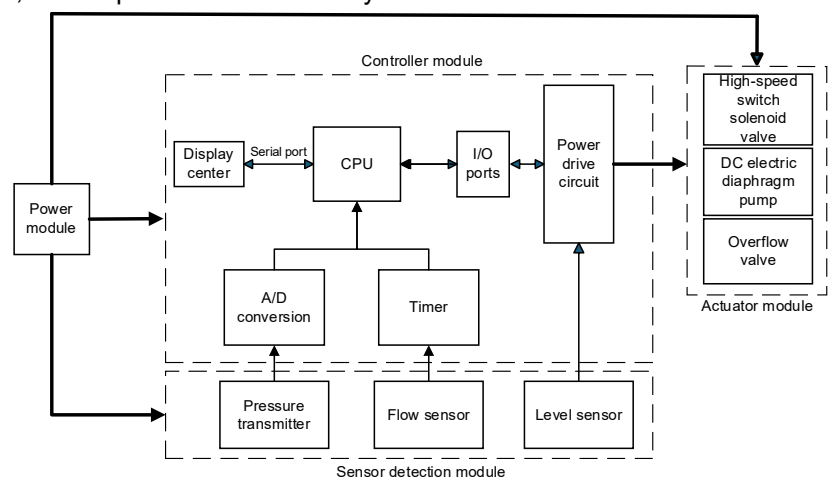


Fig. 1 - Overall system architecture diagram

## Simulation analysis

The atomization process and influence factors of atomized droplets are mainly reflected in the characteristics of liquid film breaking and atomized droplets, and the particle size and velocity of atomized droplets have a direct impact on the deposition behavior of atomized droplets (Zhang et al., 2017). In this paper, the influence of the pressure change on the particle size and the velocity of the droplets is analyzed, and, the distribution of the particle size of the droplets is also analyzed and then summarized. The distribution equation of the particle size of the droplets in the horizontal direction in the spray sector is established to describe the horizontal distribution of the particle size of the droplets under different pressures under constant flow. Through CFD simulation, the DPM model is employed to analyze the atomization performance of the nozzle under different pressures, investigate the motion velocity of droplets, and predict the particleization performance of the fan-shaped nozzle under varying pressures. This provides a certain basis for the study of droplet deposition (Sun et al., 2025; Sun et al., 2012). The spray nozzle type has a great influence on the spray droplet deposition effect, and the deposition characteristics of different types of spray nozzles are obviously different (Ma et al., 2021). In this paper, the 11001 pressure fan-shaped atomizing nozzle produced by Gegiang Plastic Hardware Co., Ltd. is selected as the chemical application unit, the spray cone angle is 110°, the working pressure is adjustable from 0.1MPa-1MPa, the equivalent aperture of the nozzle is 0.66 mm, and the spray amplitude is about 0.6 m. Under 0.3 MPa, the spray cone angle is 110°, and under other working pressures, the spray cone angle fluctuates slightly around 110°. The graphic of the 11001 pressure type of fan-shaped atomizing nozzle is shown in Fig. 2.





Fig. 2 – Nozzle diagram

Physical model and grid division: geometric modeling is carried out for the 11001 sector nozzle. The established geometric model is imported into ANSYS ICEM CFD for meshing. The computational domain of the atomization field is simplified into a cylinder 0.6 m in diameter and 0.5 m in height, the unstructured mesh is divided, and the mesh is locally densified at the nozzle, so as to improve the mesh quality and facilitate the calculation convergence. Finally, the total number of grids is 182640 and the number of nodes is 32521. The grid division is shown in Fig. 3.

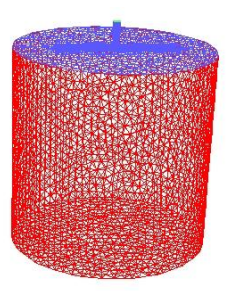


Fig. 3 - Schematic diagram of calculating the grid distribution

Discrete phase model: In Fluent, the discrete phase is assumed to be sufficiently dilute; therefore, droplet-droplet interactions are neglected, and the influence of the droplet volume fraction on the continuous phase is not considered. Therefore, in the actual process of using discrete phase simulation, the volume fraction of discrete phase shall be guaranteed to be within 10-20% (Duan et al., 2015). Assuming that the time scale of collision process is much smaller than that of ion motion, when the particle motion time is very large, the result will show a lot of time step dependence, spray rupture models include TAB model and fluctuation model, and TAB model is applicable to the flow of ground Weber number, especially for the flow problem of spray ejecting into standard atmosphere at low speed (Shu et al., 2019; Renaudo et al., 2024). Fluctuation model is applicable to the situation with Weber number greater than 100. Accurate resistance calculation is very important for the calculation of droplet motion. Fluent uses dynamic resistance model to calculate droplet resistance, which can include considering the resistance change caused by deformation of droplets.

### (1) Control equations for discrete phase particles

Fluent uses the differential equation of particle force in integral Lagrangian coordinate system to solve the orbit of discrete phase particles. Particles move along their own tracks, and when flowing, particles are affected by pressure gradient force, drag force, gravity and virtual mass force in the flow field, then, particles will change their speed along the tracks. Therefore, the motion control equation for a single particle is (Zhang et al., 2009):

$$m_k \frac{dv_k}{dt} = (\sum F)_k \tag{1}$$

where:

 $m_k$  is the mass of particle k, kg;  $v_k$  is the motion velocity of particles, m/s;  $(\sum F)_k$  is the resultant force on the particle, N.

The particle trajectory equation is:

$$\frac{dx}{dt} = u_p \tag{2}$$

The equation of motion of particles is:

$$\frac{du_p}{dt} = F_D(u - u_p) + \frac{g_x(\rho_p - \rho)}{\rho_p} + F_x$$
(3)

where:

 $u_p$  is discrete phase velocity, m/s; u is continuous phase velocity, m/s;  $\rho_P$  is the discrete phase density, kg/m³;  $\rho$  is the density of continuous phase, kg/m³;  $F_D(u-u_p)$  is the unit mass drag force of particles,  $F_D=$  $\frac{3\mu C_D R_e}{4\rho_P d_p^2}$ , N;  $d_p$  is the diameter of discrete phase, m;  $R_e$  is the relative Reynolds number,  $R_e = \frac{\rho d_p |u_p - u|}{\mu}$ .  $g_x$  is the acceleration due to gravity, m/s<sup>2</sup>;  $F_x$  denotes any additional body force per unit mass on the droplet, it is set to zero in this study.

The dynamic drag model is chosen to determine the drag coefficient through the dynamic form of droplet shape change due to the unsteady flow model involving discrete phase droplet rupture. The expression of spherical drag coefficient  $C_{ds}$  is:

$$C_{ds} = 0.424 \qquad (R_e > 1000)$$

$$C_{ds} = 0.424$$
  $(R_e > 1000)$  (4)  
 $C_{ds} = \frac{24}{R_e} (1 + \frac{1}{6} R_e^{2/3})$   $(R_e \le 1000)$  (5)

The non-spherical drag coefficient is expressed as:

$$C_d = C_{ds}(1 + 2.632y) (6)$$

where: y is the deformation value of the fog droplet, m.

Table 1

## (2) Continuous phase equation of motion

Assuming that the fluid is isothermal and there is the continuous and incompressible steady state flow of Newtonian fluid, the continuity equation is:

$$\frac{\partial \rho}{\partial t} + \frac{\partial \rho u_i}{\partial x_i} = 0 \tag{7}$$

The momentum equation is:

$$\frac{\partial \rho u_i}{\partial t} + \frac{\partial}{\partial x_i} \left( \rho u_i u_j \right) = -\frac{\partial \rho}{\partial x_i} + \frac{\partial}{\partial x_j} \left[ (\mu + u_t) \left( \frac{\partial u_i}{\partial x_j} + \frac{\partial u_j}{\partial x_i} \right) \right] \tag{8}$$

The standard k- εmodel can be characterized by the following two equations:

The *k* equation is:

$$\frac{\partial(pk)}{\partial t} + \frac{\partial(pu_ik)}{\partial x_i} = \frac{\partial}{\partial x_i} \left[ \left( \mu + \frac{u_t}{\sigma_k} \right) \frac{\partial k}{\partial x_i} \right] + G_k + G_b - \rho \varepsilon - Y_M + S_k \tag{9}$$

The  $\varepsilon$  equation is:

$$\frac{\partial (p\varepsilon)}{\partial t} + \frac{\partial (pu_{i\varepsilon})}{\partial x_i} = \frac{\partial}{\partial x_i} \left[ \left( \mu + \frac{u_t}{\sigma_{\varepsilon}} \right) \frac{\partial \varepsilon}{\partial x_i} \right] + C_{1\varepsilon} \frac{\varepsilon}{k} \left( G_k + C_{2\varepsilon} G_b \right) - C_{3\varepsilon} \rho \frac{\varepsilon^2}{k} + S_{\varepsilon}$$
(10)

where:  $G_k$  is the turbulence kinetic energy generated by velocity gradient, m<sup>2</sup>/s<sup>3</sup>;  $G_b$  is the turbulent kinetic energy generated by buoyancy, m<sup>2</sup>/s<sup>3</sup>;  $Y_M$  is the fluctuation generated by diffusion, m<sup>2</sup>/s<sup>3</sup>;  $C_1$ ,  $C_2$  and  $C_3$  are constants.

Calculation conditions and methods: due to the influence of workload, only 0.3 MPa, 5.88 mL/m (compared with working condition) and 0.5 MPa and 5.97 mL/m (system working condition) are selected for the comparative simulation experiment by fluid simulation. The simulation is carried out in Fluent, and transient calculation method is selected, without considering the impact of gravity on fog droplets. The Eulerian-Lagrange discrete phase model is selected, the fog droplet is discrete phase, the air is continuous phase, the inlet boundary condition is pressure inlet, the outlet boundary condition is pressure outlet, the collision model of wall boundary is escape model. In this study, the TAB model is employed to simulate the primary breakup of the liquid sheet, as it is well-established for low-Weber-number spray regimes. Concurrently, the standard  $k-\varepsilon$  turbulence model is adopted to resolve the continuous-phase turbulence, offering an optimal compromise between computational efficiency and predictive accuracy that has been extensively validated in spray-related flows. SIMPLE algorithm is adopted for solution, the discrete format adopts default setting, and the convergence accuracy is set as  $10^{-3}$ . The time step is set to  $1\times10^{-5}$  s and the total simulation time is 0.1 s.

## Measurement experiment and data analysis

The droplet size measurement platform built in the experiment is composed of three parts: the PWM intermittent spray system under variable pressure and flow control, the Jinan Weiner 319A laser particle size analyzer, and the linear guide slide table. Before the experiment, it is required to mask the outdoor and indoor light sources to ensure the preparation and reliability of the test results, and to adjust the laser beam of the laser particle analyzer to the spray area for later testing. In the actual variable pressure and flow control process, there will be a certain error, that is, the actual pressure value and flow value fluctuate slightly around the set value, which can be approximately regarded as stable pressure and constant flow. The system parameter settings are shown in Table 1.

System parameter settings

**Duty cycle of Duty cycle of** Spray flow rate **Pressure** solenoid valve diaphragm pump 0.3MPa 100% 2.0mL/s 34% 0.4MPa 39% 80% 2.02mL/s 0.5MPa 43% 67% 2.05mL/s 0.6MPa 51% 2.08mL/s

As shown in Fig. 4, the test under all pressure conditions takes the outlet of the nozzle as the original point, the direction perpendicular to the nozzle as x-axis, the direction right below the outlet away from the nozzle as y-axis, and the test point is located at 0.5 m right below the outlet, and the test point for determining the particle size of fog droplets is 0.05 m away from both sides respectively, until the test point is near the edge of the spray sector. The sprinkler shall repeat the measurement for 3 times at each test point under 4 pressures, i.e. there are 12 droplet size values at each test point, and there will be calculations about the average value of the droplet size at each test point under different pressures.

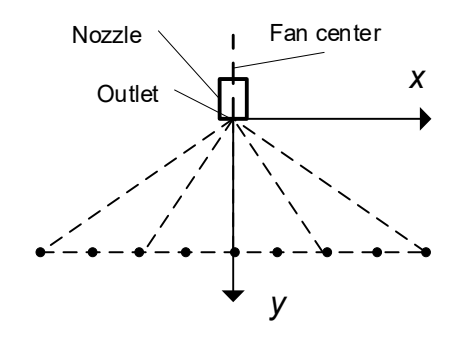


Fig. 4 - Distribution of nozzle test points

Establish the fitting function for droplet size distribution: To better analyze the droplet size distribution during spray from a fan-shaped nozzle, the horizontal position x of the test point is taken as the independent variable, and the droplet size as the dependent variable to fit the droplet size data measured under different pressures. This allows the use of a functional form to describe the droplet size distribution under varying spray pressures, where the same flow rate is achieved through the coordinated operation of a duty cycle-controlled DC electric diaphragm pump and a high-speed solenoid valve. Because of the fact that the droplet size generated by the selected fan-shaped nozzle exhibits a parabolic distribution along the horizontal direction, the droplet size distribution function is expressed as shown in Equation (11) (Wang et al., 2014):

$$y = a_1 + a_2 x + a_3 x^2 + a_4 x^3 + a_5 x^4$$
 (11)

where: x is the horizontal position, m; y is the fitting value of the droplet size,  $\mu$ m;  $a_n$  is the parameter of the distribution function (n=1, 2... 5).

Verification of function fitting properties: The fitted function models under different pressure conditions are evaluated using the coefficient of determination  $(R^2)$ , chi-square  $(\chi^2)$ , mean relative error (E), and root mean square error (RMSE). A higher fitting accuracy and model reliability are indicated when: R2 approaches 1, E is less than 10%,  $\chi^2$  and when RMSE values are smaller. The computational formulas for  $R^2$ ,  $\chi^2$ , E, and RMSE are given below (Li et al., 2017):

$$R^{2} = 1 - \frac{\sum_{i=1}^{N} (y_{i} - y_{i}')^{2}}{\sum_{i=1}^{N} (y_{i} - \bar{y})^{2}}$$
 (12)

$$\chi^{2} = \frac{\sum_{i=1}^{N} (y_{i} - y'_{i})^{2}}{N - n}$$

$$E = \frac{1}{N} \cdot \sum_{i=1}^{N} (\frac{y_{i} - y'_{i}}{y_{i}}) \times 100\%$$
(13)

$$E = \frac{1}{N} \cdot \sum_{i=1}^{N} \left( \frac{y_i - y_i'}{y_i} \right) \times 100\%$$
 (14)

$$RMSE = \sqrt{\frac{\sum_{i=1}^{N} (y_i - y_i')^2}{N}} \times 100\%$$
 (15)

where:  $y_i$  is the measurement of the droplet volume pitch diameter,  $(i = 1, 2 \cdots 13)$ ;  $y'_i$  is the predicted value of the droplet volume pitch diameter;  $\bar{y}$  is the arithmetic mean value of volume pitch diameter of the droplet; N is the number of test points; n is the number of parameters.

## Field experiment

The experiment is conducted in accordance with national standards NY/T 2667-2015 and NY/T1276-2007 (2015; 2007). In the field experiment, the spray control system of the pressure regulating and flow control is built on the spray machine frame as shown in Fig. 5 (a). Fig. 5 (b) shows the sprayer after the construction.





a) Spraver frame

b) Complete sprayer assembly

Fig. 5 - Physical map of sprayer

In the fog droplet deposition experiment, the broad bean planted in the period of flowering and podding are used as the target crops to collect the deposited fog droplets. The tested plants are located in the broad bean planting field in Xiema Town, Beibei District, Chongqing. The row spacing of the tested broad bean planting is 1.2 m, the average height is 0.514m, the ridge length is 30m, and the ground slope is about 12°. The experiment measures the deposition distribution of mist drops on the broad bean plants under the pressure of 0.3 MPa, 0.4 MPa, 0.5 MPa and 0.6 MPa. Lemon yellow is added to the clear water as the tracer, and the lemon yellow solution with a mass concentration of 2.0g/L is prepared as the spray solution for the experiment. The measurement is conducted by using a Shimadzu UV-1780 UV spectrophotometer to determine the tracer content on broad bean leaf samples for calculating spray deposition rate.

The field spraying experiment is shown in Fig. 6. The ambient temperature is 19~24 °C, the wind speed is about 1 m/s and the relative humidity is about 55~70%. When spraying, the distance between the sprinkler and the upper part of broad bean canopy is 0.50 m. According to the spacing of broad bean planting, one broad bean shall be selected every 1 m within the spray range as the test plant, 4 rows in total shall be selected, each row shall be divided into 3 sections, 5 broad beans shall be selected for each section, and 60 broad bean plants shall be selected in total. The experiment is repeated by applying one spray to each of the three segments in each row at each pressure level. Before the test, the starting position of the sprayer shall be about 5 m away from the front of the pointed broad bean plant, so as to ensure the stable working condition of the machines and tools during the sampling of fog drops. Start the sprayer and set its walking speed to 0.5m/s. After each spray application, wait for 5 minutes to allow the droplets on the leaf surfaces to dry. At each sampling point, select one leaf from the upper, middle, and lower canopy layers of each broad bean plant. From each canopy layer, collect three leaves (nine leaves in total) and place them immediately into a labeled plastic collection bag for deposition measurement. After sample collection, 30 mL of deionized water is added to each leaf sample bag, and the bag is shaken to elute the fluorescent tracer from the leaf surfaces. The concentration of the fluorescent tracer in the resulting solution is then measured using a UV spectrophotometer, and the droplet deposition is subsequently calculated.



Fig. 6 - Field spray test

# RESULTS Simulation results

The droplet particle size distribution of fan nozzle at 0.3 MPa and 0.5 MPa is shown in Fig. 7 and Fig. 8 respectively, and the droplet velocity distribution is shown in Fig. 9 and Fig. 10.

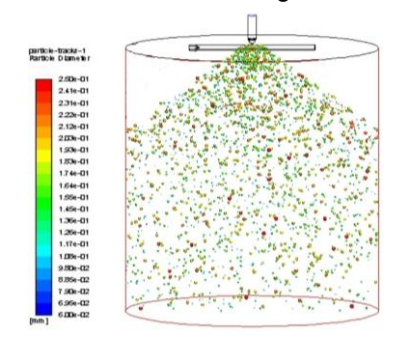


Fig. 7 - Schematic diagram of droplet size distribution at 0.3 MPa

Table 2

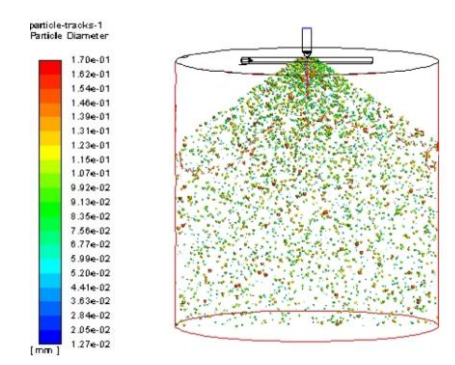


Fig. 8 - Schematic diagram of droplet size distribution at 0.5 MPa

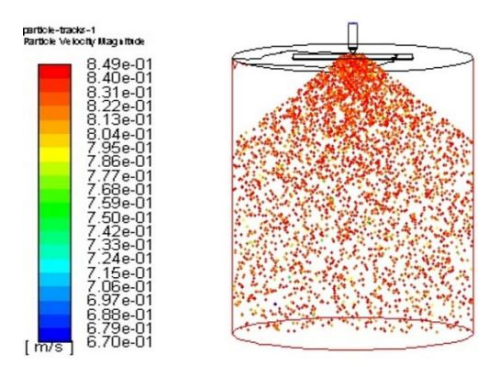


Fig. 9 - Schematic diagram of droplet velocity at 0.3 MPa

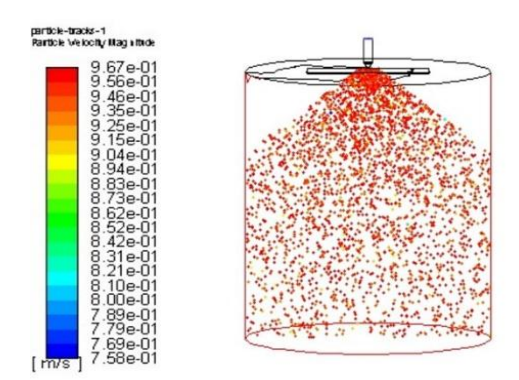


Fig. 10 - Schematic diagram of droplet velocity at 0.5 MPa

The situation can be seen from Fig. 7 and Fig. 8, about the distribution state of droplet particle size and the particle size. The particle distribution range is  $60\sim250\,\mu\text{m}$ . Compared with the droplet size under two working conditions, the droplet size under 0.5 MPa is smaller than that under 0.3 MPa, and the droplet distribution under 0.5 MPa is denser than that under 0.3 MPa. It can be seen from Fig. 9 and Fig. 10 that the maximum droplet velocity at the nozzle outlet reaches 0.849 m/s at 0.3 MPa, and that the maximum droplet velocity at the nozzle outlet reaches 0.967m/s at 0.5 MPa. In this system, when the spray flow is the same and the spray pressure is 0.5 MPa, the particle size of the spray nozzle is finer and the movement speed of the spray is faster.

## Measurement and data analysis results

It is found that the measured values of the droplet particle size at 0.4 MPa, 0.5 MPa and 0.6 MPa occasionally have a maximum or minimum value during the measurement of the droplet particle size. These distorted data are removed as interference items during the statistics. The test results are shown in Table 2.

Droplet size at different levels of spray pressure

Horizontal Droplet Size (µm) Position (m) 0.3 MPa 0.4 MPa 0.5 MPa 0.6 MPa -0.30 239.928 202.011 167.132 147.834 -0.25 204.012 179.829 139.385 123.012

Horizontal	Droplet Size (μm)						
Position (m)	0.3 MPa	0.4 MPa	0.5 MPa	0.6 MPa			
-0.20	160.124	140.322	127.673	111.367			
-0.15	127.761	108.916	100.021	84.976			
-0.10	100.01	85.221	80.114	80.113			
-0.05	80.205	74.849	73.436	66.987			
0	72.127	71.336	68.347	64.133			
0.05	82.663	74.021	73.436	69.238			
0.10	106.023	83.986	80.112	79.112			
0.15	129.141	110.352	110.352 100.466				
0.20	167.336	134.201 120.285		110.02			
0.25	208.437	208.437 182.287 138.018		122.373			
0.30	237.102	211.225	160.211	137.978			

The droplet size measurements demonstrate that droplet size decreases as spray pressure increases. The results show that the droplet size distribution across the horizontal spray direction is approximately symmetrical about the center of the spray fan, with larger droplets occurring toward the outer edges. As spray pressure increases, the lateral dispersion of the spray pattern becomes more pronounced, and the overall droplet size is significantly reduced.

### (1) Fitting of droplet size distribution functions under different spray pressures

By fitting the droplet sizes measured at various test points under different pressures, distribution functions are obtained with the droplet size as the dependent variable and with the horizontal position as the independent variable, as shown in Equations (16)-(19). The droplet size distribution functions are expressed as follows:

$$y_1 = 74.769 + 0.2579x + 0.2634x^2 - 0.0003x^3 - 9 \times 10^{-5}x^4$$
 (16)

$$y_2 = 67.634 - 0.1534x + 0.2039x^2 + 0.0003x^3 - 5 \times 10^{-5}x^4$$
 (17)

$$y_2 = 68.5 - 0.0294x + 0.1495x^2 - 8 \times 10^{-5}x^3 - 5 \times 10^{-5}x^4$$
 (18)

$$y_4 = 65.389 + 0.0816x + 0.1165x^2 - 0.0002x^3 - 3 \times 10^{-5}x^4$$
 (19)

where:

x is the horizontal position;  $y_1$  is the droplet size fitting value at 0.3 MPa;  $y_2$  is the droplet size fitting value at 0.4 MPa;  $y_3$  is the droplet size fitting value at 0.5 MPa;  $y_4$  is the droplet size fitting value at 0.6 MPa.

## (2) Model validation results under different spray pressures

This study employs SPSS software to evaluate the droplet size distribution functions under various pressure conditions by using four statistical metrics: the coefficient of determination ( $R^2$ ), chi-square statistic ( $\chi^2$ ), mean relative error (E), and root mean square error (RMSE). The complete evaluation criteria and corresponding computational results are presented in Table 3.

Distribution function fitting results

Table 3

Distribution		Fitti	ng parame	ters	Evaluation metrics				
function	<b>a</b> 1	<b>a</b> 2	<b>a</b> 3	<b>a</b> 4	<b>a</b> 5	$R^2$	χ <sup>2</sup>	Ε	RMSE
<b>y</b> 1	74.769	0.2579	0.2634	-0.0003	-9×10 <sup>-5</sup>	0.9987	5.05%	1.34%	2.02%
<b>y</b> 2	67.634	-0.1534	0.2039	0.0003	-5×10 <sup>-5</sup>	0.9943	8.69%	2.51%	3.69.%
<b>У</b> 3	68.5	-0.0294	0.1495	-8×10 <sup>-5</sup>	-5×10 <sup>-5</sup>	0.9833	9.64%	3.01%	4.47%
<i>y</i> <sub>4</sub>	65.389	0.0816	0.1165	-0.0002	-3×10 <sup>-5</sup>	0.9879	8.12%	3.06%	3.20%

The coefficient of determination ( $R^2$ ) for the droplet size distribution functions (versus horizontal position) under all pressure conditions exceeds 0.9863, approaching the ideal value of 1. The mean relative error (E) ranges between 1.34%-3.06% across pressure levels, consistently remaining below the threshold boundary of 10%. The chi-square ( $\chi^2$ ) and root mean square error (RMSE) distributions fall within the ranges of 5.05%-9.24% and 2.02%-4.47%, respectively. For evaluation metrics such as  $\chi^2$ , E, and RMSE, smaller values indicate a higher degree of overlap between experimental data points and predicted points, suggesting a good fit.

## Field experiment results

The deposition rate of fog droplets on broad bean leaves under different pressures is shown in Fig. 11. The deposition position and spray pressure have a significant influence on the deposition rate of droplets. With the increase of spray pressure, the deposition rate of droplets increases. The deposition of droplets at the upper, middle and lower heights of broad bean plants varies significantly with the particle size and velocity of droplets.

The fog droplet deposition rate in the upper canopy of broad bean plant is not significantly different from that in the middle canopy, but is significantly different from that in the lower canopy, and it increases significantly at 0.5 MPa. When spraying at 0.3 MPa, the deposition rate of fog drops on the broad bean plants is 21.1% in the upper canopy, 17.5% in the middle canopy and 13.3% in the lower canopy, with an average of 17.3%. Compared with 0.3 MPa, the droplet deposition rate increases 6.2% in the upper canopy, 13.4% in the middle canopy and 10.1% in the lower canopy, with an average increase of 9.9%; at 0.5 MPa, the deposition rate of fog droplet on the broad bean plant is 28.2% in the upper canopy, 25.3% in the middle canopy and 17.3% in the lower canopy. Compared with 0.3 MPa, the deposition rate of fog droplet on the upper canopy increases by 25.2%, 30.8% in the middle canopy and 23.1% in the lower canopy, with an average increase of 26.4%, which is the highest. Compared with 0.3 MPa, the droplet deposition rate on the broad bean plant increases by 21.9% in the upper canopy, 29.4% in the middle canopy and 17.4% in the lower canopy, with an average increase of 22.9%.

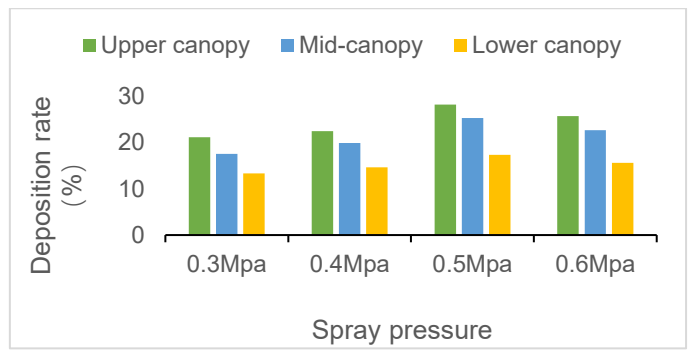


Fig. 11 – Droplet deposition rate on plants under different spray pressures

#### **CONCLUSIONS**

In this paper, the atomization characteristics of the nozzle in the PWM intermittent spray system under variable pressure and flow control are explored. CFD method is used to carry out numerical simulation, and the atomization characteristics of the nozzle under two spray pressures of 0.3 MPa and 0.5 MPa are simulated. It is verified that with the increase of spray pressure, under the premise of controlling the spray flow, the size of the droplets changes and the movement speed of the droplets increases. With 0.3 MPa as the contrast working condition, the droplet size at different horizontal positions under four pressures of 0.3 MPa, 0.4 MPa, 0.5 MPa and 0.6 MPa is tested by using a laser particle size analyzer. The experimental results indicate that the horizontal distribution of droplet size varies with spray pressure. The droplet size at 0.3 MPa is significantly larger than that at 0.6 MPa, and a pronounced change occurs around 0.5 MPa, demonstrating that increasing system pressure effectively reduces droplet size. The field experiment further confirms that improving droplet deposition is achievable by regulating spray output to produce finer droplets with greater velocity.

#### **ACKNOWLEDGEMENT**

This work was supported by the Science and Technology Research Program of Chongqing Municipal Education Commission (KJQN202202818) and the Key Scientific Research Project of Chongqing Medical and Pharmaceutical College (ygz2022403).

## **REFERENCES**

- [1] Yuan, H., Wang, G., (2015). Relationship between droplet size, coverage density and pesticide control effect (雾滴大小和覆盖密度与农药防治效果的关系). *Plant protection*, Vol. 41, pp. 9-16, Beijing/China.
- [2] Liu, Y., Jin, W., Guo, S., (2022). Study on the distribution characteristics of weeding droplets in rice field of plant protection UAV Based on variable spraying (基于变量喷施的植保无人机水稻田间除草雾滴沉积分布特性研究). *Journal of Shenyang Agricultural University*, Vol. 53, pp. 337-345, Liaoning/China.

- [3] Wongsuk, S., Qi, P., Wang, C., Zeng, A., Sun, F., Yu, F., Zhao, X., He, X., (2024). Spray performance and control efficacy against pests in paddy rice by UAV-based pesticide application: effects of atomization, UAV configuration and flight velocity. *Pest Management Science*, Vol. 80, pp.2072-2084, England.
- [4] Nukeshev, S., Tanbayev, K., Ramaniuk, M., (2024). Spray Angle and Uniformity of the Flat Fan Nozzle of Deep Loosener Fertilizer for Intra-Soil Application of Fertilizers. *AgriEngineering*, Vol.6, pp.1365-1394, Switzerland.
- [5] Koo, D., Gonalves, C. G., Askew, S. D., (2024). Agricultural spray drone deposition, Part 2: operational height and nozzle influence pattern uniformity, drift, and weed control. Weed Science, Vol.72, pp.824-832, United States.
- [6] Sapkota, M., Virk, S., Rains, G., (2023). Spray Deposition and Quality Assessment at Varying Ground Speeds for an Agricultural Sprayer with and without a Rate Controller. *AgriEngineering*, Vol.5, pp.506-519, United States.
- [7] Wang, S., Lu, D., Jonathan, V., (2024). Atomization and deposition characteristics of hydraulic nozzles for pesticide application (用于农药喷施的液力式喷头雾化与沉积分布特性分析). *Chinese Journal of Pesticide Science*, Vol. 26, pp.168-178, Jiangsu/China.
- [8] Zhang, R., L, L., Fu, W., (2019). Pulse width modulation variable control nozzle atomization performance and droplet deposition characteristics in wind tunnel environment (脉宽调制变量控制喷头雾化性能及风洞环境雾滴沉积特性). *Journal of agricultural engineering*, Vol. 35, pp.42-51, Beijing/China.
- [9] Zhang, H., Zheng, Q., Zhou, H., (2017). Study on droplet deposition distribution and off target drift during pesticide spraying (农药喷施过程中雾滴沉积分布与脱靶飘移研究). *Journal of agricultural machinery*, Vol. 48, pp.114-122, Jiangsu/China.
- [10] Sun, H., Hong, L., Wang, M., (2025). Analysis of protective effects of different ecological throw sleepers based on CFD-DPM model (基于 CFD-DPM 模型的不同生态抛枕防护效果分析). *Journal of the Yangtze River academy of Sciences*, Vol. 42, pp.19-26, Jiangsu/China.
- [11] Sun, G., Wang, X., Ding, W., (2012). Simulation analysis of droplet deposition characteristics based on CFD discrete phase model (基于 CFD 离散相模型雾滴沉积特性的模拟分析). *Journal of agricultural engineering*, Vol. 28, pp.13-19, Jiangsu/China.
- [12] Ma, Y., Gong, C., Zhang, Y., (2021). Effects of nozzle types on droplet deposition distribution and control efficacy of low-volume spray from plant protection UAV in rice canopy (喷头类型对植保无人机低容量喷雾雾滴在稻田冠层沉积分布及防治效果的影响). *Journal of Plant Protection*, Vol.48, pp.518-527, Sichuan/China.
- [13] Duan, Z., (2015). ANSYS FLUENT Fluid Analysis and Engineering Example(流体分析与工程实例) [M]. *Electronic Industry Press*, Beijing/China.
- [14] Shu, L., Yang, M., Zhao, H., (2019). Process optimization in a stirred tank bioreactor based on CFD-Taguchi method: A case study. *Journal of Cleaner Production*, Vol. 230, pp. 1074-1084, Chongqing/China.
- [15] Renaudo, C. A., Veronica, B., Bertin, D. E. (2024). Droplet deposition of agrochemical spraying: Comparison of results from a random-walk model and CFD simulations. *Canadian Journal of Chemical Engineering*, Vol.102, pp. 2082-2694, Argentina.
- [16] Zhang, S., Song, L., (2009). Simulation of atomization performance of pressure swirl nozzle (压力旋流 喷头雾化性能的仿真). *Anhui Agricultural Science*, Vol. 37, pp. 8098-8100, Hebei/China.
- [17] Wang, S., He, X., Song, J., (2014). Test Method Comparison and Distribution Function Fitting of Atomization Particle Size of Agricultural Sprinkler (农用喷头雾化粒径测试方法比较及分布函数拟合). *Journal of Agricultural Engineering*, Vol. 30, pp. 34-42, Beijing/China.
- [18] Li, B., Peng, G., Wu, S., (2017). Establishment of vacuum drying characteristics and kinetic model of konjac (魔芋真空干燥特性及动力学模型的建立). *Food and fermentation industry*, Vol. 43, pp. 115-122, Chongqing/China.
- [19] NY/T 2667. (2015). Agriculture Industry Standard of the People's Republic of China: Determination Method of Pesticide Deposition Rate.
- [20] NY/T1276. (2007). Agricultural industry standard of the People's Republic of China: General rules for safe use of pesticides.